Parlayici and Pehlivan *Journal of Analytical Science and Technology* (2019) 10:15
https://doi.org/10.1186/s40543-019-0175-3

Journal of Analytical Science and Technology

RESEARCH ARTICLE Open Access

Comparative study of Cr(VI) removal by bio-waste adsorbents: equilibrium, kinetics, and thermodynamic

Şerife Parlayici* and Erol Pehlivan

Abstract

The green adsorbents were prepared by using cranberry (*Cornus mas*) kernel shell (CKS), rosehip (*Rosa canina*) seed shell (RSS), and banana (*Musa cavendishii*) peel (BP) and were proved in removing Cr(VI). Several parameters to remove Cr(VI) such as pH, adsorbent dosage, contact time, initial Cr(VI) ions concentration, and temperature were tested. The functional groups in the matrix of CKS, RSS, and BP were detected by FT-IR for raw biomasses together with Cr(VI). The equilibrium results were inspected using four different isotherm models, with a better fitting to the Langmuir model. The maximum adsorption quantities for Cr(VI) ions were 10.42, 15.17, and 6.81 mg/g for BP, RSS, and CKS, respectively. The interrelationship coefficients were expressed by a pseudo-second-order kinetic model, assuming that the overall Cr(VI) adsorption rate is limited by the rate of adsorbate diffusion in the pores of biomass.

Keywords: Chromium(VI), Cranberry kernel shell, Rosehip seed shell, Banana peel, Adsorption

Introduction

The discharge of heavy metals into drain water through industrial actions has become a big issue for humans and aquatic lives. The most familiar toxic pollutants are chromium, lead, cadmium, copper, and mercury. Chromium as a heavy metal is one of the top 16 toxic metals that have destructive effects on human health (Wang et al. 2011). Cr(VI) is extremely toxic than Cr(III) (Sarin and Pant 2006). Cr(VI) is a strong oxidizing agent. It defectively influences the human being by oxidizing the building block of DNA and some protein molecules. The toxicity of Cr(VI) has negative effects such as skin irritation, asthma, ulceration, and severe diarrhea. It harms the kidney, circulatory tissues, liver, and nerve tissues. Disclosure to high chromium quantity causes cancer in the digestive tract and lungs (Adurty and Sabbu 2015; Ofudje et al. 2014; Gupta et al. 2016; Rengaraj et al. 2003). Therefore, extensive discharge of Cr(VI) roughly into aquatic sources of potable water has to be regulated through the enactment of legal standards and strict environmental control mechanism (Garg et al. 2004). The maximum permitted concentration limit for Cr(VI) for drinking waters that is recommended by the Environmental Protection Agency (EPA) is 0.05 mg/L. Several techniques, such as membrane process, electrochemical precipitation, electrodialysis, ultrafiltration, reverse osmosis, and ion exchange, are possible to remove harmful metals from the aquatic medium (Moosavirad et al. 2015; Pshinko et al. 2014). But, these methods are inadequate or costly when Cr(VI) is present in the wastewater at a low concentration. The adsorption technique stays the most preferred procedure because of its efficiency, non-hazardous technique, and low-priced method (Altun and Pehlivan 2012; Kaya et al. 2014). The recent adsorbents supply an attractive material, especially if the adsorbent is cheap and ready for use. As a result, we should pay close consideration to the use of natural biomass feasible in large quantities.

In recent times, many researchers have achieved the sufficient elimination of Cr(VI) from wastewater, applying natural biomasses such as rice straw (Gao et al. 2008), *Sterculia guttata* shell (Rangabhashiyam and Selvaraju 2015), Gulmohar's fruit shell (Prasad and Abdullah 2010), fish scales and egg shells (Bamukyaye and Wanasolo 2017), activated carbon derived from *Leucaena leucocephala* (Malwade et al. 2016), mangrove leaf powder (Sathish et al. 2015), garlic stem and horse

* Correspondence: serife842@hotmail.com
Department of Chemical Engineering, Konya Technical University, Campus, 42079 Konya, Turkey

Springer Open

© The Author(s). 2019 **Open Access** This article is distributed under the terms of the Creative Commons Attribution 4.0 International License (http://creativecommons.org/licenses/by/4.0/), which permits unrestricted use, distribution, and reproduction in any medium, provided you give appropriate credit to the original author(s) and the source, provide a link to the Creative Commons license, and indicate if changes were made.

chestnut shell (Parlayici and Pehlivan 2015), Juniperus procera sawdust, avocado kernel seeds and papaya peels (Mekonnen et al. 2015), and longan seed (Yang et al. 2015). The economic price of these adsorbents is insignificantly correlated to the price of ion-exchange resins or activated carbon. Most of these biomaterials consist of functional groups combined with polysaccharides, proteins, lignin, cellulose, and hemicellulose as major components. Cr(VI) uptake process is united with these functional groups (Aravind et al. 2015; Gao et al. 2008). The search for substituted advanced, cheap, eco-friendly, and sufficient biomass to replace the economically available biomasses is continuing.

In the current study, the adsorption was carried out with inexpensive CKS, RSS, and BP in the elimination of Cr(VI) from the liquid phase and was characterized using FTIR. The batch adsorption applications were implemented under different criterions like adsorbent quantity, influence time, temperature, initiative Cr(VI) concentration, and pH. Additionally, kinetic models, adsorption equilibrium isotherms, and thermodynamics were completed in this research.

Materials and methods

Equipment

UV-visible spectrophotometer (Shimadzu UV-1700) was used for the exploration of Cr(VI) amount in standard and treated solutions. pH meter (Orion 900S2) with a glass electrode and an internal reference electrode was implemented for pH measurements. Thermostated shaker of GFL 3033 model was applied for the shaking of the solutions in adsorption experiments. The FTIR spectrum was reported by using a Bruker VERTEX 70 FT-IR spectrometer.

Reagents

$K_2Cr_2O_7$, NaOH, HCl, 1-5 diphenyl carbazide, and other essential chemicals were of analytical category picked up from Merck. One thousand parts per million of a standard Cr(VI) solution was adjusted by mixing 2.835 g of potassium dichromate in 1 L distilled water. The needed initial Cr(VI) concentration was arranged by the convenient addition of pure water to the standard solution. The adsorption process was tried in the incubated shaker.

Adsorbent preparation

The CKS, RSS, and BP were obtained from the market in Konya, Turkey, and they were applied for the removal of Cr(VI) as adsorbents. BP was washed several times with pure water to eliminate the surface impurities. CKS and RSS were physically isolated from the fruit. Then, the CKS and RSS were soaked in pure water and washed several times to remove the remaining fruit. After that, CKS, RSS, and BP were dried at 60 °C for 24 h. Each biomass was crushed to increase the surface area and sieved into a particle size of nearly 125 μm. The color of the original adsorbents was completely removed when washing several times with pure water and 0.1 M HCl. All impurities related to dust and other undesirable inerts can be removed from the adsorbent surfaces by washing with diluted HCl. CKS, RSS, and BP were air-dried and stored in a desiccant and then applied for the adsorption experiments.

Adsorption experiments

The adsorption of Cr(VI) was performed by mixing (0.1 g) of CKS, RSS, and BP with Cr(VI) solution of certain concentration in a 50-ml stoppered glass flask. The flasks were horizontally agitated in an incubated agitator at 200 rpm for 60 min at 25 °C. Then, the slurry was cleaned with a filter paper to separate the adsorbent. After filtration, the concentration of the solution was analyzed by previously calibrated UV-VIS spectrophotometer at 540 nm with 1,5-diphenyl carbazide as a complexing agent. Chromium(VI) adsorption capacity per mass unit of adsorbent (q_e) was given by Eq. 1:

$$q_e = (C_0 - C_e)\ V\ m^{-1} \tag{1}$$

Cr(VI) adsorption efficiency (E %) is given by (Eq. 2):

$$E = [(C_o - C_e)/C_o] \times 100 \tag{2}$$

where C_o is the concentration of Cr(VI) ions at the initial concentration (mg L^{-1}), C_e is the concentrations of Cr(VI) ions at equilibrium concentration (mg L^{-1}), V is the volume of the aqueous phase (L), and m is amount of the adsorbent (g).

Kinetic equations were implemented for modeling the kinetics of Cr(VI) adsorption on CKS, RSS, and BP. The initial concentration of Cr(VI) solution was adjusted and placed in the flask. Then, 0.1 g of CKS, RSS, and BP were added to each flask at 298 ± 1 K, and then the solutions were agitated in a thermostat shaker at 200 rpm and original pH values was regulated to the ideal value of 2.0. The solution was filtered from the biomass at the equilibrium and was analyzed for the remaining Cr(VI) in the filtrate.

FT-IR analysis

The spectrum of CKS, RSS, and BP powder were tried to show some groups exist on the interior and exterior surface of the biomass. Figure 1 shows the FT-IR spectrum, and many functional groups were presented on the surface of adsorbents. The bands in the region of 3351 and 3294 cm^{-1} were assigned to O–H stretching (Altun et al. 2016), those at 2915 and 2933 cm^{-1} to C–H

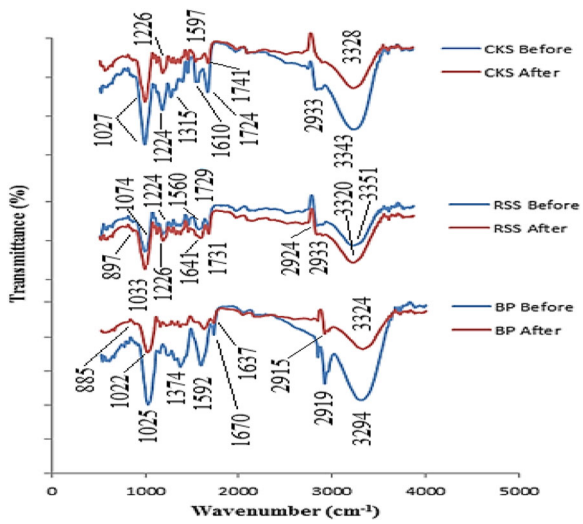

Fig. 1 FT-IR spectrum of CKS, RSS, and BP before and after Cr(VI) adsorption

stretching of alkane, and the band appearing at 1731, 1724, and 1640 cm^{-1} was referenced to the C=O bond of carboxylic acids, 1610 and 1641 cm^{-1} to C–O stretches of ester or ether. Aromatic C–O stretching vibrations of the lignin component and –C–O–C– stretching appearing at 1025, 1027, and 1033 cm^{-1}, respectively (Noeline et al. 2005; Kumar et al. 2010). The weak band in the region of 885 and 889 cm^{-1} was attributed to N–H deformation of amino groups. Looking at the spectrum, it shows carboxylic acid, and hydroxyl groups showed a dominant role in the removal of Cr(VI) ions. Some clear shifts from the matrix of the adsorbents were seen after the adsorption of Cr(VI). These were a changing of wavenumber from 3343 cm^{-1} (CKS) to 3323 cm^{-1} (Cr(VI)-loaded CKS), from 3351 cm^{-1} (RSS) to 3320 cm^{-1} (Cr(VI)-loaded RSS), and from 3294 cm^{-1} (BP) to 3324 cm^{-1} (Cr(VI)-loaded BP). The number of –OH groups in the dominant form in the structure of the adsorbents was decreased by interaction with Cr(VI). This caused the decrease in the intensity of the band and changed the existing band to a narrow band spectrum. FT-IR analysis of the adsorbents displayed that some bands shifted after Cr(VI) adsorption. The following are for CKS: the band in 1724 cm^{-1} to 1741 cm^{-1}, the band in 1610 cm^{-1} to 1597 cm^{-1}, and the band in 1224 cm^{-1} to 1226 cm^{-1}; the following are for RSS: the band in 2924 cm^{-1} to 2933 cm^{-1}, the band in 1729 cm^{-1} to 1731 cm^{-1}, the band in 1560 cm^{-1} to 1641 cm^{-1}, the band in 1224 cm^{-1} to 1226 cm^{-1}, and the band in 1074 cm^{-1} to 1033 cm^{-1}; and the following are for BS: the band in 2919 cm^{-1} to 2915 cm^{-1}, the band in 1670 cm^{-1} to 1637 cm^{-1}, the band in 1592 cm^{-1} to 1614 cm^{-1}, and the band in 1025 cm^{-1} to 1022 cm^{-1}. Changes in the band frequencies in the FT-IR spectrum correspond to the changes in the energy levels of the functional groups. The shifts in the FT-IR spectrum proved the complexation of Cr(VI) with functional groups existing in the biomass. Similar results were obtained by Aravind et al. (2015) and Brungesh et al. (2015).

Results and discussion

Influence of pH

The elimination of Cr(VI) by CKS, RSS, and BP at different pH values of adsorption is shown in Fig. 2. The pH of the solution is a basic control parameter for the elimination of Cr(VI). The pH of these solutions was adjusted to 1.5–6.0 with diluted HCl and NaOH solutions. The Cr(VI) concentration, contact time, and adsorbent dose were kept constant (50 ppm, 10 g/L, and 60 min, respectively).

Figure 2 shows that the optimum elimination efficiency and adsorption capacity of Cr(VI) ions were higher at low pH. Cr(VI) adsorption increased at pH value of 2. The biomass surface can be protonated at low pH values. The positively charged ions existed on the surface of the adsorbent in acidic medium, and Cr(VI) can interact with the matrix of biomass by electrostatic interaction and complexion.

In acidic medium, the equilibrium can be demonstrated as follows:

$$HCr_2O_7 \rightarrow H^+ + Cr_2O_7^{2-}$$

$$H_2CrO_4 \rightarrow H^+ + HCrO_4^-$$

The equilibrium in basic condition is given as follows:

$$Cr_2O_7^{2-} + OH^- \rightarrow HCrO_4^- + CrO_4^{2-}$$

$$HCrO_4^- + OH^- \rightarrow CrO_4^{2-} + H_2O$$

It is probable that 1 mol of dichromate ion reacted with 2 mol of (–OH) ions present in the solution. At low

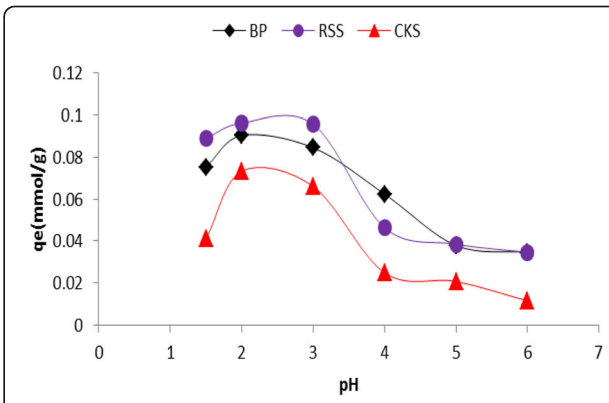

Fig. 2 Effect of pH on the adsorption of Cr(VI) by BP, RSS, and CKS (adsorption conditions: concentration of Cr(VI), 50 ppm; adsorbent dosage, 10 g/L; contact time, 1 h; temperature, 25 ± 1 °C; $\lambda = 540$ nm)

pH values, the adsorption capacity was better. This can be a result of the formation of a large number of H^+ ions at low pH environments. They neutralize the negatively charged hydroxyl groups (–OH) ions present on the matrix of biomass which causes the increasing hindrance to diffusion of positively charged dichromate ions. The functional groups present in the biomasses are efficient to hold Cr(VI) on the surface of biomass. Cr(VI) ion was converted to Cr(III) in the acidic environment, with the protons removed in the functional groups of the biomass, and was engaged in the adsorbent surface. The high protonated CKS, RSS, and BP of surfaces could easily coordinate with the oxyanion ($Cr_2O_7^{2-}$) present in the solution through electrostatic interaction (Gorzin and Bahri Rasht Abadi 2018). The maximum percent removal of Cr(VI), i.e., 93.83%, 99.96%, and 76.2% by BP, RSS, and CKS, were observed at pH 2.0, and all other experiments were done at this pH. The similar pH-depended trend was also observed by some other researchers for the Cr(VI) removal by various biosorbents (Bai and Abraham 2001; Goyal et al. 2003; Bai and Abraham 1998; Bishnoi et al. 2004).

At lower pH values, there was a formation of more polymerized chromium oxide species (Bai and Abraham 2001), which results in a decrease in Cr(VI) removal. When increasing the pH values from 2 to 6, the $HCrO_4^-$ gradually converts to the divalent CrO_4^{2-}. As the pH increases, the surface of biosorbent becomes more negatively charged. The number of positively charged sites decreased. This causes increased repulsion between Cr(VI) and biomass. The negative surface charges on the biomass matrix do not provide the adsorption of anions due to the electrostatic repulsion (Hiremath and Theodore 2016). The CKS, RSS, and BP surfaces protonated in the acidic situation, and electrostatic interactions were generated between the biomass surface and Cr(VI). For this reason, adsorption became more in the acidic conditions and the optimum pH value was found as 2.

Effect of contact time

Figure 3 shows the influence time on Cr(VI) adsorption by CKS, RSS, and BP at 25 °C and initial pH 2. The duration of adsorption was adjusted as 5, 15, 30, 60, 120, 240, 480, 720, 1080, and 1440 min. For the equilibrium study, the elimination of Cr(VI) increased from 0.072 to 0.090 mmol/g by BP, 0.081 to 0.095 mmol/g by RSS, and 0.062 to 0.075 mmol/g by CKS. The adsorption capacity increased immediately in the first 30 min, and the rate of adsorption decreased subsequent stages and then attained a plain value then remained stable. Initially, many empty surface sites may be usable for the adsorption. During the adsorption period, the vacant sites remaining on the surface of the biomass may be hard to bind due to repellent forces between Cr(VI) and the slurry (Saravanane et al. 2002). In Fig. 3, it can be easily seen that a plateau value was reached in 90 min for CKS, whereas for RSS and BP, the steady state condition arrived in 60 min.

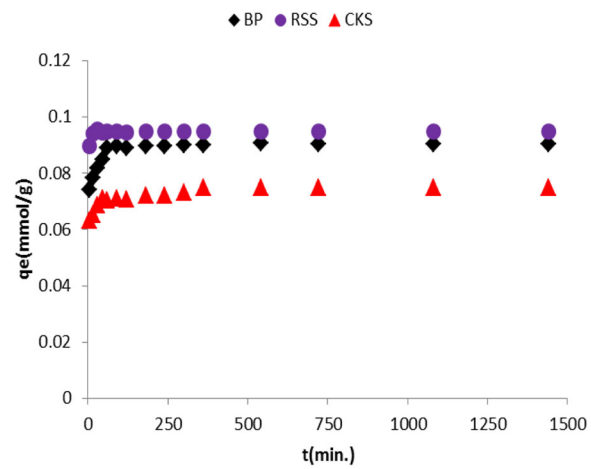

Fig. 3 Effect of contact time on adsorption of Cr(VI) by BP, RSS, and CKS (adsorption conditions: concentration of Cr(VI), 50 ppm; pH 2; adsorbent dosage, 10 g/L; temperature, 25 ± 1 °C; λ = 540 nm)

Influence of adsorbent dosage

The adsorption of Cr(VI) onto CKS, RSS, and BP were studied by varying the adsorbent quantity (2.5, 5, 7.5, 10, 12.5, 25 g/L) in the initial Cr(VI) concentration (50 ppm), temperature (25 °C), and pH 2.

Figure 4 shows the retention of Cr(VI) ions against the amount of adsorbent. As shown in the graph, the adsorbent amount increased while the adsorption of Cr(VI) ions increased, and then a certain value was reached. After a certain amount, the adsorption did not change

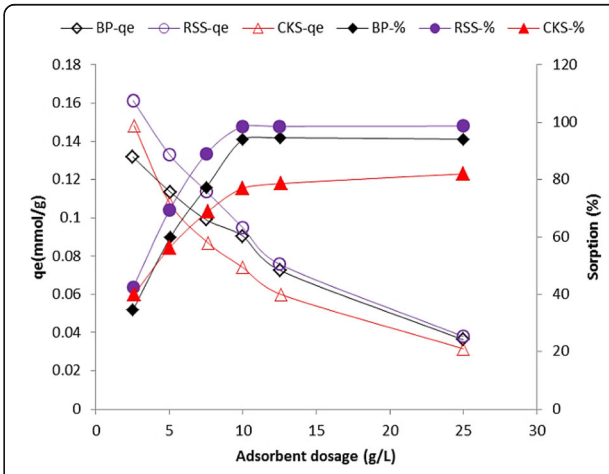

Fig. 4 Effect of adsorbent dosage on adsorption capacity and percentage removal of Cr(VI) ions on the adsorption of Cr(VI) by BP, RSS, and CKS (adsorption conditions: concentration of Cr(VI), 50 ppm; pH 2; contact time, 1 h; temperature, 25 ± 1 °C; λ = 540 nm)

significantly and the stability of Cr(VI) on the biomass was attained at an adsorbent dose of 10 g/L. At equilibrium, the percent removal became constant probably because of the saturation of the available adsorption sites (Khan et al. 2017). The percentage adsorption of Cr(VI) was observed as 34.55% at 2.5 g/L and 94.15% at 25 g/L with the adsorbent dose of BP. When adsorption dose rose from 2.5 g/L to 25 g/l, the percentage changed from 42.47% to 98.70% with RSS, and in case of CKS, it was observed from 39.94% to 82.01%. The results showed that a slow increase in Cr(VI) elimination was observed after an adsorbent amount of 10 g/L for BP, RSS, and CKS. However, Cr(VI) adsorption capacity values showed a reverse trend. Adsorption capacities were found as 0.13, 0.16, and 0.14 mmol/g, for BP, RSS, and CKS, respectively.

Adsorption isotherms

Cr(VI) adsorption experiments were carried out at different starting Cr(VI) ion concentrations (from 5 to 100 ppm), and adsorption capacities were calculated. When the equilibrium was reached, Cr(VI) ions that adsorbed and remained in the solution phase were measured and their compatibility with Freundlich, Langmuir, Scatchard, and D-R adsorption isotherms was investigated. The isotherm parameters and the regression coefficients (R^2) corresponding to each model are given in Table 1.

These isotherm equations are as follows:

Freundlich Eq. (3):

$$q = K_f C_e^n \tag{3}$$

where n is the heterogeneity factor, and K_f is the adsorption constant, q is the weight adsorbed per unit weight of adsorbent, and C_e is the metal concentration in bulk solution at equilibrium. Taking logs and reorganizing, the Eq. (4) was acquired.

$$\log q_e = \log K_f + \frac{1}{n} \log C_e \tag{4}$$

The Freundlich equation of K_f and n values is calculated. K_f values were 3.53, 3.92, and 5.16 L/g, for CKS, RSS, and BP, respectively. The slope $1/n$ measures the surface heterogeneity. The values of $1/n$ were 0.72, 0.77, and 0.69, for CKS, RSS, and BP, respectively. The value for $1/n$ below 1 indicates a normal Freundlich isotherm.

Langmuir Eq. (5):

$$\frac{C_e}{q_e} = \frac{1}{K_b A_S} + \frac{C_e}{A_S} \tag{5}$$

where A_s and K_b are coefficients, C_e is the metal concentration in bulk solution at equilibrium, and q_e is the biomass capacity. The maximal biomass capability for holding Cr(VI) was determined as 15.17 mg/g with RSS, while it was 6.81 and 10.42 mg/g with CKS and BP, respectively. It has been suggested that for favorable adsorption, the values of the dimensionless separation factor R_L should be $0 < R_L < 1$ (Eq. 6).

$$R_L = \frac{1}{1 + K_L C_o} \tag{6}$$

The value of R_L represents whether adsorption is favorable ($0 < R_L < 1$), unfavorable ($R_L > 1$), linear ($R_L = 1$), or irreversible ($R_L = 0$). In the present study, the values of R_L were 0.0955, 0.0138, and 0.117, supporting a favorable adsorption.

Scatchard isotherm is a widely used technique in assessing the affinity of binding section taking a part in a specific adsorption process. For adsorption from solution, the Scatchard model expressed as Eq. (7).

$$q_e / C_e = Q_s K_s - q_e K_s \tag{7}$$

where K_s (L/mg) and Q_s (mg/g) are the adsorption isotherm parameters of Scatchard. For Cr(VI) adsorption, the Scatchard curve was plotted, and from the equation, Q_s and K_s constant values were obtained and are given in Table 1. The calculated R^2 value 0.99 supports the appropriateness of Langmuir isotherms for CKS, RSS, and BP. Dubinin–Radushkevich (D–R) isotherm is generally applied to illuminate the sorption isotherms of a single dissolved mixture. The D–R isotherm, at a distance from being an equivalent of the Langmuir isotherm, is broader than the Langmuir isotherm as it discards the homogeneous surface or constant adsorption potential. For adsorption from solution, the D–R isotherm model expressed as Eq. (8).

$$\ln q_e = \ln q_m - \beta \varepsilon^2 \tag{8}$$

where ε represents Polanyi potential in Eq. (9). The constant β indicates the mean free energy.

Table 1 Parameters of Langmuir, Freundlich, Scatchard, and D-R isotherms for adsorption of Cr(VI) on 252 BP, RSS, and CKS

Adsorbent	Langmuir			Freundlich			D-R				Scatchard		
	Q_m	b	R^2	K_f	n	R^2	X_m	K	E_{ad}	R^2	Q_S	K_S	R^2
BP	10.42	0.095	0.984	0.88	1.39	0.971	0.0015	0.006	9.05	0.984	13.33	0.067	0.705
RSS	15.18	0.716	0.991	5.83	1.31	0.982	0.0052	0.005	9.81	0.992	15.42	0.701	0.958
CKS	6.82	0.075	0.963	0.49	1.44	0.938	0.0009	0.006	8.84	0.963	8.86	0.049	0.799

Table 2 Cr(VI) removal using a variety of low-cost adsorbents

Adsorbent	Adsorption capacities (mg/g)	Reference
Mango kernel activated carbon	7.8	Rai et al. 2016
Rice straw	3.15	Gao et al. 2008
Gulmohar's fruit shell	12.28	Prasad and Abdullah 2010
Wood apple shell	13.74	Sartape et al. 2010
Egg-shells	10.3	Bamukyaye and Wanasolo 2017
Ficus auriculata leaves powder	13.33	Rangabhashiyam and Selvaraju 2015
Pre-boiled sunflower stem	4.9	Jain et al. 2009
papaya peels	7.160	Mekonnen et al. 2015
avocado kernel seeds	10.08	Mekonnen et al. 2015
Cranberry kernel shell	**6.81**	*Present work*
Rosehip seed shell	**15.17**	*Present work*
Banana peel	**10.42**	*Present work*

$$\varepsilon = \mathrm{RT.In}\left(1 + \frac{1}{C_e}\right) \tag{9}$$

E is the adsorption per molecule of the adsorbate when it is transported to the surface of the biomass from infinity in the liquid phase and can be computed using Eq. (10):

$$E = (2K)^{-1/2} \tag{10}$$

The convenience of the equilibrium curve for the Langmuir isotherm was investigated. Adsorption energy (E_{ad}) was determined 9.05, 9.81, and 8.84 kJ/mol for BP, RSS, and CKS, respectively. The experimental results of our investigation revealed that BP has the highest sorption capacity. Many workers have tried various waste biomasses for Cr(VI) ion adsorption. The correlation of biomass capacity with the different biomasses reported in the references is given in Table 2 and compared with CKS, RSS, and BP. The experimental data of the current investigations are comparable with the reported values. The results showed that the maximum adsorption capacity obtained in this study was higher compared to other low-cost adsorbents.

Thermodynamics of adsorption

Thermodynamic applications of an adsorption system are to understand whether the system is spontaneous or not. The adsorption of Cr(VI) onto CKS, RSS, and BP was easily carried out at different temperatures (25 °C, 35 °C, 45 °C, and 55 °C) for thermodynamic analysis. The experimental data obtained were used to calculate Gibbs free energy change (ΔG°), entropy change (ΔS°), and enthalpy change (ΔH°) from Eqs. (11, 12).

$$\Delta G^{\circ} = -\mathrm{RT}\ \ln K_C \tag{11}$$

$$\Delta G^{\circ} = \Delta H^{\circ} - T\Delta S^{\circ} \tag{12}$$

R is universal gas constant (8.314 J mol^{-1} K^{-1}), T is temperature (K), and K_C is equilibrium constant. The calculated results are reported in Table 3.

The negative value of ΔH° indicates that the adsorption reaction is exothermic. The negative value of the standard entropy change reflects a decreasing in the variability at the biomass/solution interface throughout the elimination process. ΔG° values were found to be negative. The negative ΔG^{o} values with temperature suggest that the mechanism is appropriate and spontaneous nature of adsorption with a high preference for Cr(VI) onto CKS, RSS, and BP.

Adsorption kinetics

To identify the mechanism of adsorption, some kinetic models have been applied and the possible rate-controlling step that consists of mass transport and a chemical reaction was determined for explaining the mechanism. Pseudo-first- and pseudo-second-order models are suitable for chemical kinetics. The kinetics of the adsorption of Cr(VI) can be described by the pseudo-first-order equation and is usually given as (Eq. 13):

Table 3 Thermodynamic parameters

	ΔS°	ΔH°	ΔG° (J mol-1)				
Adsorbent	J $K^{-1}mol^{-1}$	J mol^{-1}	T=298.15K	T=308.15K	T=318.15K	T=328.15K	R^2
BP	-132.15	-48039.2	-8639	-7318	-5997	-4675	0.996
RSS	-220.03	-77869.1	-12268	-10068	-7867	-5667	0.999
CKS	-71.37	-26700.4	-5419	-4706	-3992	-3279	0.925

Table 4 Kinetic parameters

Adsorbent	C_o(ppm)	Pseudo First-order			Pseudo Second-order		
		k_1	qe(ppm)	R^2	k_2	qe(ppm)	R^2
BP	50	0.0184	1.07	0.9371	0.087	4.76	0.999
RSS	50	0.0009	2.37	0.3439	1.51	4.94	1.000
CKS	50	0.0159	0.50	0.7769	0.24	3.74	0.998

$$\ln(q_e - q_t) = \ln q_e - k_1 t \quad (13)$$

k_1 is the rate constant of pseudo-first-order adsorption, and q_e and q_t are the adsorption capacities (mg/g) of Cr(VI) at equilibrium and at a time (t). The pseudo-second-order adsorption kinetic rate equation is indicated as:

$$\frac{t}{q_t} = \frac{1}{k_2\, qe^2} + \frac{t}{q_e} \quad (14)$$

$$h = k_2 q_e \quad (15)$$

k_2 is the rate constant of pseudo-second-order adsorption ($g\,mg^{-1}\,min^{-1}$), and h ($mg\,g^{-1}\,min^{-1}$) is the initial adsorption rate. The kinetic parameters were determined and given in Table 4.

The acquiescence between laboratory results and the applied standard parameters were compared with the correlation coefficients (R^2). The results showed that the regression coefficient (R^2) values of Cr(VI) adsorption was closer to 1, indicating that the most of the adsorption followed the pseudo-second-order kinetic model and it signifies that "chemisorption" took place during the reaction for all concentrations of Cr(VI). The rate constants were illustrated in Table 1. The equilibrium capacities were calculated from the pseudo-second-order model which is closely accepted by the capacities found from the isotherm studies.

Conclusions

In this research, the elimination of Cr(VI) from the bulk phase was completed by using three biomasses (CKS, RSS, and BP). The adsorption relied on pH, adsorbent dose, and contact time. The maximum elimination for Cr(VI) from the liquid phase succeeded at pH 2.0. The equilibrium interrelated with four adsorption isotherm equations. The increase in the adsorbent mass causes an increase in Cr(VI) adsorption zone numbers due to the adsorption of Cr(VI).

Optimum removal of Cr(VI) was accomplished at a biomass amount of 10 g/L. The equilibrium isotherm models stated that the adsorption pattern of Cr(VI) ions in BP, RSS, and CKS followed the Langmuir model as well as Dubinin–Radushkevich (D–R) isotherm model. By applying the Langmuir model equation, the maximum Cr(VI) adsorption capacity of BP, RSS, and CKS were found to be 10.42, 15.17, and 6.81 mg/g, respectively. RSS showed the highest Cr(VI) capacity in all biomasses. The rate constants for adsorption were calculated from the Lagergren equation.

Abbreviations

BP: Banana (*Musa cavendishii*) peel; CKS: Cranberry (*Cornus mas*) kernel shell; RSS: Rosehip (*Rosa canina*) seed shell

Acknowledgements

Not applicable.

Funding

Not applicable.

Availability of data and materials

Research data have been provided in the manuscript.

Authors' contributions

EP conceived of the study and contributed in design and organization of the manuscript. ŞP carried out the adsorption and kinetic experiments and performed the data analysis. EP did the manuscript writing and executed the data interpretation. All authors read and approved the final manuscript.

Competing interests

The authors declare that they have no competing interests.

Publisher's Note

Springer Nature remains neutral with regard to jurisdictional claims in published maps and institutional affiliations.

Received: 5 December 2018 Accepted: 25 March 2019
Published online: 06 April 2019

References

Adurty S, Sabbu JR. Novel catalytic fluorescence method for speciative determination of chromium in environmental samples. J Analy Sci Tech. 2015;6(1):7.

Altun A, Pehlivan E. Removal of Cr (VI) from aqueous solutions by modified walnut shells. Food Chem. 2012;132:693–700.

Altun T, Parlayıcı S, Pehlivan E. Hexavalent chromium removal using agricultural waste rye husk. Desal Water Treat. 2016;57:17748–56.

Aravind J, Kanmani P, Devisri AJ, Dhivyalakshmi S, Raghavprasad M. Equilibrium and kinetic study on chromium (VI) removal from simulated waste water using gooseberry seeds as a novel biosorbent. Glob J Envir Sci Manag. 2015; 1(3):233–44.

Bai SR, Abraham TE. Studies on biosorption of chromium (VI) by dead fungal biomass. J Sci Ind Res. 1998;57:821–4.

Bai SR, Abraham TE. Biosorption of Cr (VI) from aqueous solution by Rhizopus nigricans. Bio Tech. 2001;79:73–81.

Bamukyaye S, Wanasolo W. Performance of egg-shell and fish-scale as adsorbent materials for chromium (VI) removal from effluents of tannery industries in Eastern Uganda. Open Acc Lib J. 2017;4(8):1.

Bishnoi NR, Bajaj M, Sharma N. Adsorption of Cr (VI) from aqueous and electroplating wastewater. Envir Tech. 2004;25:899–905.
Brungesh KV, Nagabhushana BM, Raveendra RS, Krishna HR, Prashantha PA, Nagabhushana H. Adsorption of Cr (VI) from aqueous solution onto a mesoporous carbonaceous material prepared from naturally occurring Pongamia pinnata seeds. J Envir Anal Toxic. 2015;5(6):1.
Gao H, Liu Y, Zeng G, Xu W, Li T, Xia W. Characterization of Cr (VI) removal from aqueous solutions by a surplus agricultural waste rice straw. J Hazar Mater. 2008;150(2):446–52.
Garg VK, Gupta R, Kumar R, Gupta RK. Adsorption of chromium from aqueous solution on treated sawdust. Bio Tech. 2004;92:79–81.
Gorzin F, Bahri Rasht Abadi MM. Adsorption of Cr (VI) from aqueous solution by adsorbent prepared from paper mill sludge: kinetics and thermodynamics studies. Ads Sci Techn. 2018;36(1–2):149–69.
Goyal N, Jain SC, Banerjee UC. Comparative studies on the microbial adsorption of heavy metals. Adv Envir Res. 2003;7:311–9.
Gupta VK, Chandra R, Tyagi I, Verma M. Removal of hexavalent chromium ions using CuO nanoparticles for water purification applications. J Coll Inter Sci. 2016;478:54–62.
Hiremath PG, Theodore T. Zirconium-doped fungal sorbents: preparation, characterization, adsorption isotherm, and kinetic and mathematical modelling study for removal of fluoride. Adv Chem. 2016;1–14.
Kaya K, Pehlivan E, Schmidt C, Bahadir M. Use of modified wheat bran for the removal of chromium (VI) from aqueous solutions. Food Chem. 2014;158: 112–7.
Khan TA, Nazir M, Ali I, Kumar A. Removal of chromium (VI) from aqueous solution using guar gum–nano zinc oxide biocomposite adsorbent. Arab J Chem. 2017;10:2388–98.
Kumar GV, Ramalingam P, Kim MJ, Yoo CK, Kumar MD. Removal of acid dye (violet 54) and adsorption kinetics model of using musa spp. waste: a low-cost natural sorbent material. Korean J Chem Eng. 2010;27:1469–75.
Malwade K, Lataye D, Mhaisalkar V, Kurwadkar S, Ramirez D. Adsorption of hexavalent chromium onto activated carbon derived from Leucaena leucocephala waste sawdust: kinetics, equilibrium and thermodynamics. Inter J Envir Sci Techn. 2016;13(9):2107–16.
Mekonnen E, Yitbarek M, Soreta TR. Kinetic and thermodynamic studies of the adsorption of Cr (VI) onto some selected local adsorbents. Sou African J Chem. 2015;68:45–52.
Moosavirad SM, Sarikhani R, Shahsavani E, Mohammadi SZ. Removal of some heavy metals from inorganic industrial wastewaters by ion exchange method. J Wat Chem Tech. 2015;37(4):191–9.
Noeline BF, Manohar DM, Anirudhan TS. Kinetic and equilibrium modelling of lead (II) sorption from water and wastewater by polymerized banana stem in a batch reactor. Sep Pur Tech. 2005;45:131–40.
Ofudje EA, Awotula AO, Oladipo GO, Williams OD. Detoxification of chromium (VI) ions in aqueous solution via adsorption by raw and activated carbon prepared from sugarcane waste. Cov J Phy Life Sci. 2014;2(2):110–22.
Parlayici S, Pehlivan E. Natural biosorbents (garlic stem and horse chestnut shell) for removal of chromium (VI) from aqueous solutions. Environ Monit Asses. 2015;187(2):1–10.
Prasad AG, Abdullah MA. Biosorption of Cr (VI) from synthetic wastewater using the fruit shell of gulmohar (Delonix regia): application to electroplating wastewater. NC State University, Bioresources. 2010;5(2):838–53.
Pshinko GN, Puzyrnaya LN, Yatsyk BP, Kosorukov AA, Goncharuk VV. Removal of Cr (VI) from aqueous solutions by calcined Zn/Al-and Mg/Fe-hydrotalcites. J Water Chem Tech. 2014;36(6):257–64.
Rangabhashiyam S, Selvaraju N. Adsorptive remediation of hexavalent chromium from synthetic wastewater by a natural and ZnCl2 activated Sterculia guttata shell. J Mol Liq. 2015;207:39–49.
Rengaraj S, Joo CK, Kim Y, Yi J. Kinetics of removal of chromium from water and electronic process waste water by ion exchange resins: 1200H, 1500H and IRN97H. J Hazar Mater. 2003;102:257–75.
Saravanane R, Sundararajan T, Sivamurthyreddy S. Efficiency of chemically modified low cost adsorbents for the removal of heavy metals from wastewater. A comparative study. Indian J Envir Heal. 2002;44:78–81.
Sarin V, Pant KK. Removal of chromium from industrial waste by using Eucalyptus bark. Bio Tech. 2006;97:15–20.
Sathish T, Vinithkumar NV, Dharani G, Kirubakaran R. Efficacy of mangrove leaf powder for bioremediation of chromium (VI) from aqueous solutions: kinetic and thermodynamic evaluation. App Wat Sci. 2015;5(2):153–60.
Wang Q, Song J, Sui M. Characteristic of adsorption, desorption and oxidation of Cr (III) on birnessite. Energy Pro. 2011;5:1104–8.
Yang J, Yu M, Chen W. Adsorption of hexavalent chromium from aqueous solution by activated carbon prepared from Longan seed: kinetics, equilibrium and thermodynamics. J Ind Eng Chem. 2015;21:414–22.

Submit your manuscript to a SpringerOpen journal and benefit from:

- ► Convenient online submission
- ► Rigorous peer review
- ► Open access: articles freely available online
- ► High visibility within the field
- ► Retaining the copyright to your article

Submit your next manuscript at ► springeropen.com